Applied Energy 88 (2011) 4785–4794

Contents lists available at ScienceDirect

Applied Energy

journal homepage: www.elsevier.com/locate/apenergy

A model predictive control strategy for load shifting in a water pumping scheme with maximum demand charges ☆

Adam Jacobus van Staden, Jiangfeng Zhang *, Xiaohua Xia

Centre of New Energy Systems, Department of Electrical Electronic and Computer Engineering, University of Pretoria, Pretoria 0002, South Africa

ARTICLE INFO

Article history:
Received 29 November 2010
Received in revised form 10 June 2011
Accepted 14 June 2011
Available online 26 July 2011

Keywords:
Demand side management
Maximum demand
Model predictive control
Optimal control
Water pumping

ABSTRACT

This paper defines and simulates a closed-loop optimal control strategy for load shifting in a plant that is charged for electricity on both time-of-use (TOU) and maximum demand (MD). A model predictive control approach is used to implement the closed-loop optimal control model, and the optimization problem is solved with integer programming. The simulated control model yields near optimal switching times which reduce the TOU and MD costs. The results show a saving of 5.8% for the overall plant, and the largest portion of the saving is due to a reduction in MD. The effect of disturbances, model uncertainty and plant failure is also simulated to demonstrate the benefits of a model predictive control model.

1. Introduction

Load shifting is an aspect of demand side management (DSM) where electricity demand is shifted out of peak demand periods to off-peak demand periods. To encourage load shifting utilities have structured electricity tariffs with time-of-use (TOU) and/or maximum demand (MD) charges [1–3]. MD charges are also used by utilities to represent infrastructure costs due to high peak demands.

TOU charges are based on higher kWh rates during high demand periods, whilst MD charges are based on fixed fees per maximum kVA or kW for a month in high demand periods (e.g., during the day). MD is measured as the highest average demand in kVA or kW during any integrating period – the integrating period is generally 30 min, and it coincides with the TOU periods [1,2]. The MD charge is typically applied to an integration period with the highest average consumption in an entire month. For example, the maximum average kVA in a 30 min period might be consumed in the morning on the first day of the month. This means that customers are encouraged to move load out of high demand periods and to spread the load evenly throughout the whole month.

Various techniques have been used to solve load shifting problems in different applications. For example, fuzzy logic is used in Ref. [4] for load shifting of a domestic hot water cylinder, a neural network is used in Ref. [5] for load shifting in a petrochemical plant, in Refs. [6–13] load shifting problems are modeled as optimization problems, and in Refs. [14–17] load shifting problems are modeled as optimal control problems [18].

Note that the optimization techniques used in Refs. [6–13] do not consider external disturbances or inaccurate system models. In other words, no feedback and subsequent re-optimization is included to compensate for these deficiencies. From a control theory point of view [19], these types of applications can be referred to as open loop control models, because no feedback is used to determine if the controller's input has achieved the desired output. This means that the system does not observe the output of the processes that it is controlling.

The optimization techniques (open loop optimal control models) used in Refs. [6–13] are valuable starting points to quantify the potential for load shifting, but they cannot actively control a load shifting process with disturbances. To actively control a load shifting process a controller with feedback and subsequent re-optimization is required. This type of controller is referred to as a closed-loop optimal controller [19].

The load shifting techniques in Refs. [6–17] can be further categorized as follows: Refs. [6–8] consider optimization (open loop optimal control) with TOU charges, Refs. [9–13] consider optimization (open loop optimal control) with TOU and MD charges, Refs. [14,15] consider closed-loop optimal control models with TOU

☆ A preliminary version of the paper was presented at the IEEE PowerTech Conference, Bucharest, Romania, 28 June–2 July 2009.

* Corresponding author.
E-mail addresses: vanstad@gmail.com (A.J. van Staden), zhang@up.ac.za (J. Zhang), xxia@postino.up.ac.za (X. Xia).

0306-2619/$ - see front matter © 2011 Elsevier Ltd. All rights reserved.
doi:10.1016/j.apenergy.2011.06.054

Nomenclature

n	the nth pump, and $n = 1, \ldots, N$
N	the total number of pumps
t	the tth discrete switching interval, and $t = 1, \ldots, T$
T	the total number of discrete switching intervals
u_{tn}	the binary switching status of the nth pump at the tth switching interval; $u_{tn} = 0$ when the pump is off and $u_{tn} = 1$ when the pump is on
r	the rth reservoir, and $r = 1, \ldots, R_0$
R_0	the total number of reservoirs
L_{tr}	the level of the rth reservoir at the tth switching interval
A_{rn}	the flow rate of the nth pump at the rth reservoir
B_r	the constant inflow or outflow rate of the rth reservoir, e.g., gravitational flow
S	the total number of switching intervals in an MD integrating period
s	the sth switching interval in any MD integrating period, and $s = 1, \ldots, S$
p_n	the power consumption of the nth pump
c_t	the TOU energy cost in the tth switching interval
z_n	the nth MD integer variable for the nth pump, and $0 \leqslant z_n \leqslant S$
C	the MD charge in R/kW or R/kVA, and 'R' represents the South African currency called Rand (US \$1 $\approx$ R 7.00)
λ_1	the weight assigned to the TOU energy cost
λ_2	the weight assigned to the MD cost
H	the control horizon

charges and only Refs. [16,17] consider closed-loop optimal control models with TOU and MD charges. Furthermore, the closed-loop optimal control models in Refs. [16,17] are re-optimized daily, but should ideally be re-optimized more frequently to react to disturbances closer to real-time.

Therefore, little evidence could be found to prove the applicability of closed-loop optimal control for load shifting in different applications, and specifically where both TOU and MD charges are considered.

Furthermore, the switching intervals in Refs. [9–13,16,17] are greater than or equal to the MD integrating period. This means that optimization within the MD integrating period is not considered. This paper shows that smaller switching intervals can reduce MD costs.

The aim of this paper is to define and simulate a closed-loop optimal control model for a specific plant that is charged on both TOU and MD. A model predictive control (MPC) approach [20] with integer programming (IP) optimization [21] is selected to model and simulate the closed-loop model.

An MPC strategy is selected, because the periodic re-optimization characteristic provides stability during external disturbances. The periodic re-optimization also compensates for inaccurate or simplified system models [22].

This paper is organized as follows. In Section 2 a generic discrete time linear optimal control model is defined [23,24]. In Section 3 this generic optimal control model is applied to a case study. In Section 4 the applied optimal control model is simulated and the results are compared with the current control model of the case study. Concluding remarks and recommendations are covered in Section 5.

2. Generic Control Model for a water pumping scheme

2.1. Definition and benefits of an MPC strategy

MPC is a closed-loop optimal control approach that uses an explicit model of the plant to predict future response (outputs). The basic structure of the MPC approach is shown in Fig. 1.

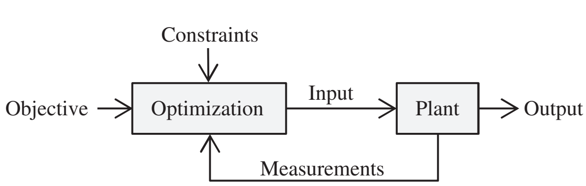

Fig. 1. Structure of an MPC model (adapted from Ref. [20]).

With an MPC approach an open loop optimal control problem is solved repeatedly over a finite control horizon at each switching interval, and only the first control step (input) is implemented after each iteration. At the next sampling interval (iteration) the state of the plant is re-sampled (measured) and the process of optimization is repeated [20,22].

This means that an optimization algorithm is executed at each switching interval to determine the optimal control input for the plant. Optimization of electricity costs is an example of an optimization objective in a water pumping scheme.

Furthermore, the periodic re-sampling (feedback) and optimization provide stability against disturbances and inaccurate system modeling. For example, real time changes in water demand or inaccurate flow assumptions.

The first step required to define a generic closed-loop MPC optimal model for a water pumping scheme is to define a generic open loop optimal control model. This is covered in Section 2.2. The second step is to convert the open loop model to a closed-loop MPC model. This is covered in Section 2.3. Note that the closed-loop MPC optimal control approach is explained further within the context of a water pumping scheme in Section 2.3.

2.2. Generic open loop optimal control model

Various references were used as a basis to define a generic open loop optimal control model for a water pumping scheme [11,12,16,17,25–28]. The state model of the generic open loop optimal control model is defined as

$$L_{(t+1)r} = L_{tr} + \sum_{n} A_{rn} \cdot u_{tn} + B_r. \tag{1}$$

The aim is to optimize the switching of a number of pumps (N) to reduce the cost of both TOU and MD charges over a control horizon (H), for example 24 h. The objective function to minimize is defined as

$$\min_{u_{tn}} \left\{ \lambda_1 \sum_{n=1}^{N} \left(\sum_{t=1}^{T} u_{tn} \cdot p_n \cdot c_t \right) + \lambda_2 \max \left\{ C \sum_{n=1}^{N} \sum_{t=1+k\cdot S}^{k\cdot S+S} u_{tn} \cdot p_n, \qquad k = 0, \ldots, \left(\frac{T}{S} - 1 \right) \right\} \right\}. \tag{2}$$

The first part of (2) represents the energy cost, whilst the second part represents the MD cost. Due to the definition of the MD cost in (2) the objective function is nonlinear. Therefore, an extra variable z_n and extra constraints (4) are introduced to remove the nonlinear maximum function in (2). The linear objective function is defined as

$$\min_{u_{tn}, z_n} \sum_{n=1}^{N} \left(\lambda_1 \sum_{t=1}^{T} u_{tn} \cdot p_n \cdot c_t + \lambda_2 \frac{p_n}{S} \cdot z_n \cdot C \right), \tag{3}$$

where z_n represents the nth MD integer variable for the nth pump, and $0 \leqslant z_n \leqslant S$. The variables u_{tn} and z_n need to be solved by the optimization algorithm over the control horizon (H).

The variable z_n counts the maximum number of switching intervals that the nth pump is switch on during any MD integrating period. Note that the technique to represent the MD costs with a variable in the objective function is based on Ref. [17]. In this paper the variables u_{tn} and z_n are modeled as binary integer and pure integer variables respectively, whilst in Ref. [17] all the variable are modeled as continuous variables. The benefit of the integer variables is that it avoids a second scheduling step within the MD period.

The following constraints are required to force z_n to represent the highest MD across all MD integrating periods:

$$\sum_{n=1}^{N} \left(\sum_{t=1+k \cdot S}^{k \cdot S+S} u_{tn} \cdot p_n - p_n \cdot z_n \right) \leqslant 0 \qquad \text{for } k = 0, \ldots, \left(\frac{T}{S} - 1 \right), \tag{4}$$

where k represents the number of MD periods in the control horizon. In other words, the purpose of (4) is to constrain each individual MD period to the maximum value of the MD that is represented by z_n in the objective function in (3).

The relationship between the variables in (2)–(4) is shown in Fig. 2. Fig. 2 shows that a control horizon is divided into T switching intervals, and each MD interval consists of one or more switching intervals (S). For example, if a control horizon (H) of 24 h is divided into 15 min switching intervals, then the total number of switching intervals is 96 (T = 96). This means that each MD interval is divided into two switching intervals (S = 2) if the MD integrating intervals are 30 min long. If the first pump in this example runs for only one switching interval in any MD integrating period then z_1 = 1.

The reservoir level constraints are defined as

$$D_r \leqslant L_{tr} \leqslant E_r, \tag{5}$$

where D_r represents the minimum level constraint of the rth reservoir and E_r represents the maximum level constraint of the rth reservoir.

2.3. Generic closed-loop MPC optimal control model

The closed-loop MPC optimal control model is defined with the same state model as the open loop optimal control model in (1), and the objective function is defined as

$$\min_{u_{tn}, z_n} \sum_{n=1}^{N} \left(\lambda_1 \sum_{t=1+m}^{T+m} u_{tn} \cdot p_n \cdot c_t + \lambda_2 \frac{p_n}{S} \cdot z_n \cdot C \right), \tag{6}$$

where $m = 1, \ldots, M$, and M represents the last switching interval of the controller. The last switching interval could be considered as infinite unless the controller is stopped. The formulation of (6) is based on [22].

In (6) the open loop optimal control problem is solved repeatedly over a finite control horizon (H) at each switching interval t, and only the first control step u_{tn} is implemented after each iteration. At the next sampling interval (t + 1) the state of the plant (L_{tr}) is re-sampled and the process of optimization is repeated over the new control horizon [m, $m + T$].

The same constraints for the open loop model in (4) and (5) apply to the closed-loop MPC model. The only difference is that the constraints need to be updated after each switching interval is implemented.

The MPC control strategy can be explained further with Fig. 3, which shows the result of a hypothetical controller that controls the level of one reservoir. The reservoir has a constant inflow rate and the outflow is controlled with only one pump.

The control model in Fig. 3 uses 15 min switching intervals (S = 2), and a control horizon (H) of 8 h. Fig. 3 shows the level of the reservoir L_{t1} (output), the statuses of the pump u_{t1} (inputs) and the TOU energy charges (c_t) over 14 h.

Fig. 3 shows that the current time is 6 h which means that the inputs and output prior to 6 h are historical and the inputs and output after 6 h are the future predicted values. Note that the MPC sampling intervals are chosen to coincide with the switching intervals of the pumps.

The process of the MPC controller in Fig. 3 can be described as follows: At the current time (6 h) the controller samples the current reservoir level, applies all the constraints, and predicts the future statuses of the pump that will optimize cost over the next 8 h. The calculated statuses of the pump are referred to as the predicted inputs (u_{t1}). The results in Fig. 3 show that the pump needs to be switched on for the next 15 min (6 h–6 h 15 min), and that pump needs to be switched on for a few more 15 min intervals between 10 h and 14 h. Fig. 3 also shows how the level of the reservoir is predicted over the next 8 h from 6 h to 14 h.

However, once the predicted inputs are calculated only the first predicted input is implemented and the rest of the predicted inputs are discarded. After the first predicted input is implemented the entire optimization process is repeated. This means that the pump is switched on for 15 min, and when the 15 min interval lapses the level of the reservoir is sampled again, the constraints are re-applied and the future statuses of the pump over the next

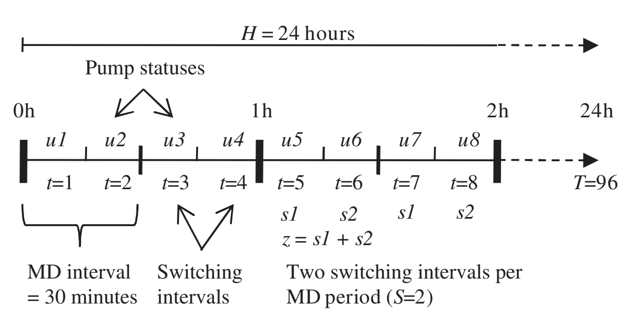

Fig. 2. Relationships between control variables.

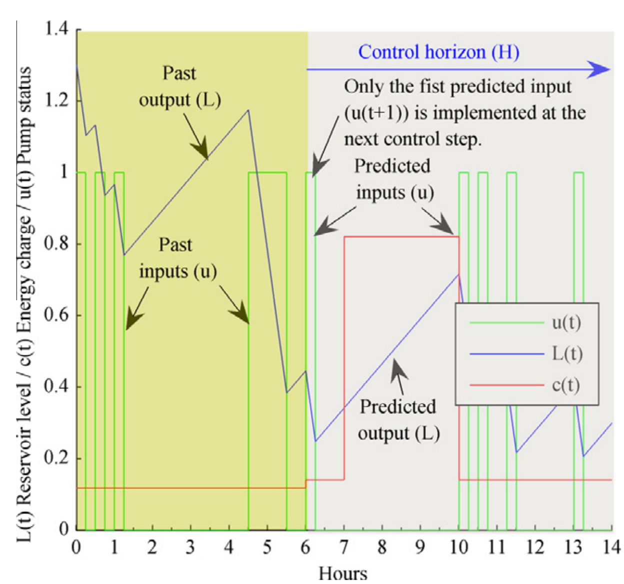

Fig. 3. MPC strategy; only the first predicted input is implemented (adapted from Ref. [20]).

8 h are predicted again. When the new statuses of the pump are determined only the first status (predicted input) is implemented again. Therefore, the optimization process repeats indefinitely at each switching interval (t).

3. Application of the Generic Control Model to a case study

3.1. Plant overview

A water purification plant in the Tshwane municipality in South Africa is selected for the case study. The plant can be divided into the purification plant itself and the pumping scheme of the purified water (see Fig. 4). This paper focuses on the water pumping scheme, because it consumes the bulk of the electricity and it has potential for load shifting.

Water flows from the dam through the purification plant into a reservoir ($R1$) at 40 ML/day (mega liter per day). $R1$ is also supplied with water from a fountain at 5 ML/day. $R1$ has a capacity of 1.4 ML.

The water from $R1$ is pumped to two reservoirs: $R2$ and $R3$, with a capacity of 120 ML and 60 ML respectively. The water to $R2$ is pumped by motors K1, K2 and K3; each rated at 300 kW with the ability to pump 22 ML/day per motor. The water to $R3$ is pumped by motors G1, G2 and G3; each rated at 275 kW with the ability to pump 10 ML/day per motor.

The primary source of water to $R2$ and $R3$ is a water utility in the province called Randwater, and $R3$ is also supplied by boreholes at a rate of 10 ML/day.

The remainder of this section focuses on the water pumping scheme at the purification plant, which includes reservoir $R1$ and motors K1, K2, K3, G1, G2 and G3.

The constraints of $R1$ and the relevant pumps are:

(1) At least one of the pumps to both $R2$ and $R3$ must run continuously, otherwise the water in the pipes flows back into $R1$.
(2) As much water as possible must be pumped to $R3$, because the reservoir is small and therefore the risk of running out of water is high.

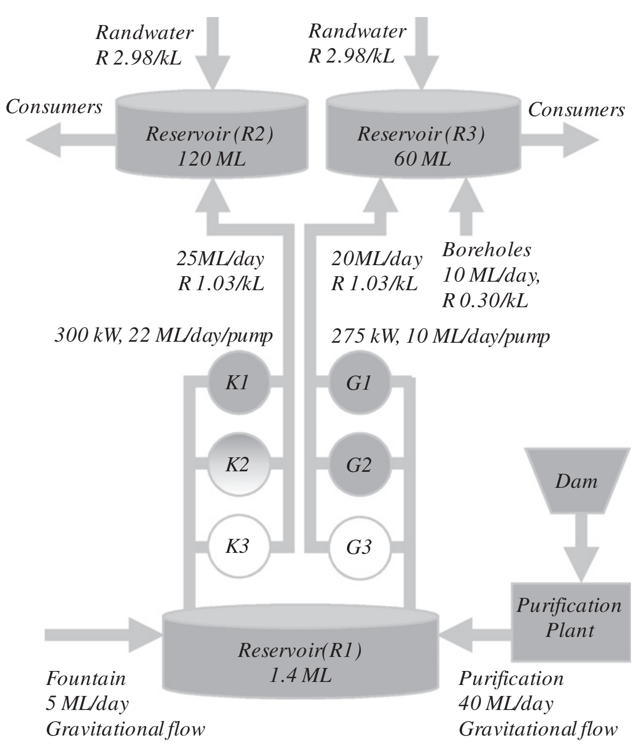

Fig. 4. Pumping scheme of the water purification plant.

(3) Running three pumps to either $R2$ or $R3$ is not desirable, because the mechanical losses are too high.
(4) A motor should not be started more than three times per hour.
(5) Randwater supplies most of the water to $R2$ and $R3$ at a cost of R 2.98/kL (Rand per kilolitre). The boreholes and the purification plant are used as alternative water supplies with significant lower costs, i.e., R 0.30/kL and R 1.03/kL respectively. This means that the maximum amount of water from $R1$ must be pumped to $R2$ and $R3$, irrespective of the electricity costs –including peak electricity periods.
(6) This also means that there is no imposed limit on the amount of water that can be pumped from the purification plant to $R2$ and $R3$, because the demand of water from $R2$ and $R3$ is larger than the supply from the purification plant.

The pumps K1, K2, K3, G1, G2 and G3 are currently controlled with a level based control system. This means that each pump switches on and off when $R1$ reaches a specific level. The current switching levels are shown in Table 1. Based on the on/off switching levels in Table 1, G1, G2 and K1 are running most of the time, whilst K2 switches on and off to control the level. The exception is during outages when the level of $R1$ may drop into the switching ranges of the other pumps. Note that K3 and G3 are used as back-up pumps. As a result this configuration pumps approximately 25 ML/day to $R2$ and 20 ML/day to $R3$, as shown in Fig. 4.

Therefore, the most viable load shifting option for the pumping scheme at the purification plant, within the listed constraints, and without large infrastructure expenditure, is the switching times of K2. The problem with the current switching times of K2 is that K2 operates approximately six times per day, for more than 30 min at a time. This means that the maximum demand per month equals the maximum capacity of the motors. With the current control model K2 could also operate during peak demand periods, because the motor simply starts when the reservoir level is too high. Therefore, it would be more desirable if K2 can run more frequently, for shorter periods, and preferable not during peak demand periods.

Therefore, the requirement for the control model is to determine the optimal switching statuses for K2 that minimizes electricity cost for both TOU and MD charges. The control models must also be able to compensate for external disturbances and inaccurate system modeling. As explained, a closed-loop MPC optimal control strategy satisfies this requirement.

This means that a simple on/off control strategy is not feasible. Firstly the on/off strategy would not be an optimal solution, unless an open loop (optimization) strategy is used to determine the optimal on/off statuses. Secondly, if an open loop (optimization) strategy is used, the solution would not be able to compensate for disturbance or an inaccurate system modeling.

3.2. Electricity tariff

The purification plant is supplied with electricity from the Tshwane municipality on the standard 11 kV bulk supply tariff. This tariff includes a flat energy charge and an MD charge [2].

Table 1
Switching levels of motors in the Rietvlei pumping scheme.

Pump	Current "on" level	Current "off" level	Revised "off" level
K1	0.6	0.3	0.05
K2	1.3	0.9	0.2
K3	Back-up		
G1	0.8	0.4	0.1
G2	1.0	0.7	0.15
G3	Back-up		

However, for this case study the municipality's 11 kV TOU tariff is used instead. The 11 kV TOU tariff includes a TOU and an MD charge [2]. The TOU tariff is used instead of the current flat energy charge to demonstrate the benefit of load shifting. The variable fees of the TOU tariff for September 2008 are summarized in Table 2.

3.3. Current electricity costs

The calculated electricity cost of the overall pumping scheme over 30 days is shown in Table 3. The overall cost calculation is required to determine the overall saving for the plant.

The simulated energy cost for K2 from Section 4 is used in Table 3, whilst the energy cost for K1, G1 and G2 is calculated with the high demand (winter) TOU tariff. A uniform load throughout the month is assumed in the calculations. The calculated results in Table 3 correlates with the actual consumption for the plant during June 2008 where an MD of 1152 kVA was registered with a total energy consumption of 640416 kWh.

3.4. Revising of the switching levels

To enable more effective load shifting of K2 the "off" switching levels of all the motors are revised to allow K2 with a wider operating band. The revised switching levels are shown in Table 1. Based on the revised switching levels G1, G2 and K1 will still run most of the time, whilst K2 switches on and off to control the level.

3.5. Assumptions for the control models

(1) The revised switching levels from Table 1 is used.
(2) Only K2 is considered in the optimal control model. Pumps K1, K3, G1, G2 and G3 are assumed to be controlled with the existing level based control model, which (as explained) results in K1, G1 and G2 to always run.
(3) The high demand season (winter) tariffs are used.
(4) The off-peak, standard and peak times for all days are considered the same as a week day. This is to simplify simulation over a 30 day period.
(5) A motor power factor of one is used for the simulations. This means the kVA and kW consumption is equal.

Table 2
Summary of the Tshwane 11 kv TOU tariff.

Period	Cost
Off-peak (0 h–6 h and 22 h–24 h)	
High demand (winter)	0.1187 R/kWh
Low demand (summer)	0.1049 R/kWh
Standard (6 h–7 h and 10 h–18 h)	
High demand (winter)	0.1411 R/kWh
Low demand (summer)	0.1383 R/kWh
Peak (7 h–10 h and 18 h–22 h)	
High demand (winter)	0.8205 R/kWh
Low demand (summer)	0.2628 R/kWh
Maximum demand charge (applicable in peak and standard times)	66.50 R/kVA

(6) A utilization factor of one is used for the simulations. This means that the motors run at full load.
(7) The pumping scheme consumes more than 90% of the electricity of the total plant, and therefore the overall cost saving is evaluated against the consumption of the pumping scheme only.

3.6. Formulation of the control models

(1) *Current level based control model*: The current level based control model is also defined as a discrete time model, which is based on the state model in (1). Since there is only one reservoir ($R1$) and one pump (K2) to consider, the level of reservoir $R1$ at the t-th switching interval is defined as

$$L_{t+1} = L_0 + \sum_{t=1}^{t} FLOWIN_t - FLOWOUT_t \cdot u_t, \tag{7}$$

where L_0 is the initial level of reservoir $R1$, and $t = 1, \ldots, T$. The upper level limit is used as the initial level, i.e., L_0 = 1.3 ML. $FLOWIN_t$ is the relative inflow to $R1$ over the tth switching interval, which is a constant flow from the fountain and the purification plant, minus the outflows from the level controlled motors, i.e., $FLOWIN_t$ = purification plant + fountain − G1 − G2 − K1 = 3 ML/day. $FLOWOUT_t$ is the outflow of K2 for the tth switching interval, which is a constant value of 22 ML/day.The control status of the pump (K2) is based on the revised switching levels, and it is defined as

$$u_t = \begin{cases} 0, & \text{when } L_t \leqslant 0.2\text{ ML} \\ 1, & \text{when } L_t \geqslant 1.3\text{ ML} \end{cases}. \tag{8}$$

(2) *Open loop optimal control model with IP optimization*: Since there are only one reservoir ($R1$) and one pump (K2) to be considered, the state model in (7) also applies to the open loop optimal control model, and the generic objective function in (3) is simplified as

$$\min_{u_t, z} \left(\lambda_1 \sum_{t=1}^{T} u_t \cdot p \cdot c_t + \lambda_2 \frac{p}{S} \cdot z \cdot C \right), \tag{9}$$

where C = R 66.50 for the maximum kVA/kW over any 30 min integrating period, p = 300 kW, S = 2, T = 2HS, and $\lambda_1 = \lambda_2 = 1$. Setting $\lambda_1 = \lambda_2 = 1$ means that the total cost in (9) represents actual costs with no preference between a TOU or MD reduction. Note that since only one pump is considered, variables p_n and z_n are represented as p and z in Eq. (9).The objective function in (9) is subject to the constraints in (11)–(13).

Based on Table 2, the cost of energy in Rands for the high demand season is defined as

$$c_t = \begin{cases} 0.1187/2S, & t \in [0, 12S] \cup [44S, 48S] \\ 0.1411/2S, & t \in [12S, 14S] \cup [20S, 36S] \\ 0.8205/2S, & t \in [14S, 20S] \cup [36S, 44S] \end{cases}. \tag{10}$$

The generic level constraints in (5) are defined as the upper and lower level constraints as

$$L_t \leqslant 1.3\text{ ML} \qquad \text{for } t = 1, \ldots, T, \tag{11}$$

and

Table 3
Calculated electricity costs of the overall pumping scheme over 30 days.

Pump	kWh	MD (kVA)	Energy cost (R)	MD cost(R)	Total costs (R)
K1 calculated	216,000	300	59,438	19,950	79,388
K2 simulated	30,348	300	8351	19,950	28,301
G1 calculated	198,000	275	54,485	18,288	72,772
G2 calculated	198,000	275	54,485	18,288	72,772
Total	642,348	1150	176,758	76,475	253,233

$$L_t \geqslant 0.2\ \text{ML} \qquad \text{for } t = 1, \ldots, T. \tag{12}$$

The generic MD constraints in (4) (applicable in peak and standard times) are simplified defined as

$$\sum_{t=1+k\cdot S}^{k\cdot S+S} u_t \cdot p - p \cdot z_s \leqslant 0 \qquad \text{for } k = 0, \ldots, \left(\frac{T}{S} - 1\right). \tag{13}$$

Note that the constraint of the number of allowable starts per hour for K2 is automatically adhered to as part of the optimization, i.e., K2 will be switched on at most once per MD period, which results in a worst case of two starts per hour.

The optimization problem is solved with IP, because the variables u_t and z are defined as binary integer and pure integer variables.

(3) *Open loop optimal control model with linear programming (LP) optimization*: If the integer variables (u_t and z) in the open loop optimal control model (9)–(13) are treated as real variables, then the optimization problem becomes a linear programming problem. This strategy is not practical for the selected case study, because the pumps are binary controlled. However, the LP optimization strategy is included as a benchmark to evaluate the effectiveness of the IP solutions.

The LP solution is considered as a benchmark, because the variables are not constrained to integers, which results in one optimal result that satisfies all the constraints. The LP optimization also solves very quickly (less than 10 s).

Therefore, the result from the LP optimization is better or equal to the result form the IP optimizations, which provides a possible least bound for the objective function value evaluated at integer feasible solutions.

The definition of the open loop control model with LP optimization is the same as the open loop optimal control model with IP optimization in the previous subsection. The only difference is that u_t and z are not constrained to integer values –u_t is only constrained as $0 \leqslant u_t \leqslant 1$.

(4) *Closed-loop MPC optimal control model with IP optimization*: The closed-loop MPC optimal control model is defined with the same state model as the current control model and the open loop optimal control model in (7).

Since there is only one pump (K2) and one reservoir (*R*1) to consider, the generic closed loop objective function in (6) is simplified as

$$\min_{u_t, z} \left(\lambda_1 \sum_{t=1+m}^{T+m} u_t \cdot p \cdot c_t + \lambda_2 \frac{p}{S} \cdot z \cdot C \right). \tag{14}$$

The objective function in (14) is minimized subject to the constraints in (11)–(13) over the prediction horizon [m, $m + T$], as described in Section 2.3. This means that the closed-loop MPC model is not a simple optimization problem, but a series of optimization solutions with iterative implementations of obtained solutions.Note that the TOU cost function in (10) applies to the objective function in (14) as well.

3.7. Simulation environment

(1) *Choice of simulation timeout*: The simulation timeout value for the IP optimizations in this case study is selected as 10 s. In the initial simulations it was found that a longer timeout has no effect on the MD cost and a negligible effect on the TOU energy costs. For example, the TOU energy costs of the plant reduced by only 0.03% with simulation timeouts between 2 and 24 h. This result was for a specific simulation scenario with an open loop optimal control model with IP optimization ($H = 24, S = 2$). A simulation timeout is important in a closed-loop MPC optimal control model where the optimization cannot run indefinitely, i.e., a less optimal solution that satisfies the constraints in a practical timeframe is preferred.
(2) *Choice of switching intervals*: The switching intervals are chosen to coincide with the TOU and MD periods, i.e., at least one switching interval per 30 min MD integrating period ($S = 1$). To reduce the MD charge S needs to be bigger than one ($S > 1$), which divides the MD integrating period into smaller intervals. However, the size of S is a trade-off between computational time, equipment constraints and cost saving. For this paper a value of $S = 2$ has been selected.
(3) *Choice of control horizon*: Like the switching interval, the control horizon (H) is a trade-off between computational time and cost saving. The control horizon in this paper is selected as 24 h (i.e. $H = 24$).
(4) *Solving the problem with Matlab and LPSOLVE*: The current control model and the optimal control models are simulated with Matlab [29].

The IP optimization problem is solved with the Matlab and LPSOLVE [30]. LPSOLVE is an open source library that is callable from Matlab and it solves IP problems. LPSOLVE is selected, because it provides good performance with many variables within reasonable optimization times. LPSOLVE uses a branch and bound strategy with LP relaxation to solve the IP optimization problem [30,31].

The following LPSOLVE settings are used in the IP simulations to improve performance: the bound on the objective function is set to 15,000 for the open loop and closed-loop MPC simulations; the tolerance on the integers is selected as 0.01; and the timeout on the optimization is selected as 10 s.

The LP optimization problem is solved with the Matlab LP function (*linprog*).

The LPSOLVE and *linprog* functions can be used to solve the following minimization problem:

$$\min_{x} f^T \cdot x \text{ such that } A \cdot x \leqslant b \text{ and } Aeq = beq, \tag{15}$$

where f, b, and beq are vectors; A and Aeq are matrices; and the solution x is an integer vector for *bintprog* and a decimal vector for *linprog*. In the LPSOLVE simulations the values of x that represent u_t are constrained to binary integers, whilst the value of x that represents z is constrained to a pure integer.

4. Results

4.1. Comparison of the control models

This subsection simulates and compares the control models that are defined in Section 3. This comparison includes:

(1) The current level based control model.
(2) The open loop optimal control model with LP optimization.
(3) The open loop optimal control model with IP optimization.
(4) The closed-loop MPC optimal control model with IP optimization.

The main objective of this subsection is to prove that the closed-loop MPC optimal control model reduces both TOU and MD costs, and that the closed-loop MPC model is just as effective as the open loop control model when there are no disturbances, system model inaccuracies, or plant failures.

Table 4 shows the costs and savings of the overall plant for each simulated scenario, and Fig. 5 shows savings from Table 4 in a graphical format. Note that the overall calculated cost from

Section 3 is used to determine the saving of the overall plant in Table 4 and Fig. 5.

(1) *Current control model –the baseline*: The current control model is simulated over a 30 day period with 15 min switching intervals ($S = 2$). The current model is simulated with the revised switching band for K2 as defined in Table 1 and (8). The energy and MD costs for the current control model are shown in Table 4.

Fig. 6 shows the results of the current control model on the 30th day. The 30th day is selected, because it is a good example where K2 switches on in peak times, i.e., in Fig. 6 K2 runs for 2½ h in peak time and a ½ h in standard time.

(2) *Open loop optimal control model with LP optimization – the benchmark*: The open loop LP optimal control model is simulated over a 30 day period. The reservoir level at the end of each day is used as the initial reservoir level for the next day. Fig. 7 shows the simulated results of the open loop LP optimal control model with S=2 and H=24 on the first day.

The load in Fig. 7 is moved out of the peak energy charge periods, and the load in the standard energy charge periods is reduced. The MD is also reduced by spreading the load evenly over the applicable 30 min MD periods, i.e., peak loads during the applicable MD periods are minimized.

The monthly energy and MD costs for this scenario are shown in Table 4. Fig. 5 (Table 4) shows that this scenario results an MD saving of 7.17% and a TOU energy saving of 1.84%. This gives a total saving (MD and TOU) of 9.01%.

As mentioned, the open loop LP model is not considered as a control solution for the specific case study, because the pumps are binary controlled, i.e., it is only a benchmark for comparisons.

Table 4
Comparison of the savings with the simulated control models.

	Current model – baseline	Open-loop with LP – benchmark	Open-loop with IPa	Closed-loop MPC with IPa
Energy cost	R 176,758	R 172,101	R 172,158	R 172,175
MD Cost	R 76,475	R 58,306	R 66,500	R 66,500
Total costs	R 253,233	R 230,407	R 238,658	R 238,675
Energy saving	0.00%	1.84%	1.82%	1.81%
MD saving	0.00%	7.17%	3.94%	3.94%
Total saving	0.00%	9.01%	5.76%	5.75%

Simulated over 30 days, with $H = 24$, $S = 2$, and timeout = 10 s.

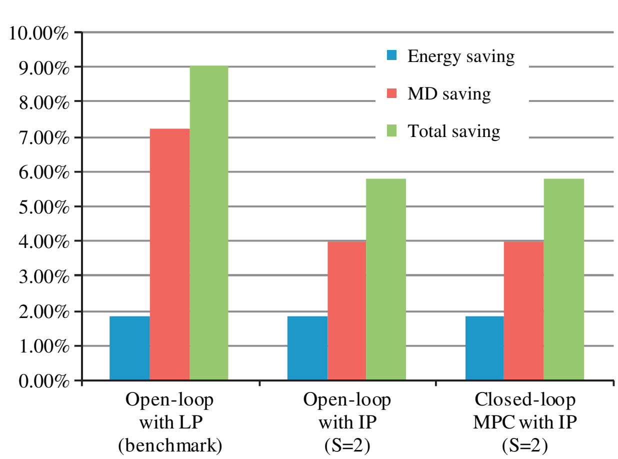

Fig. 5. Comparison of the savings with the simulated control models.

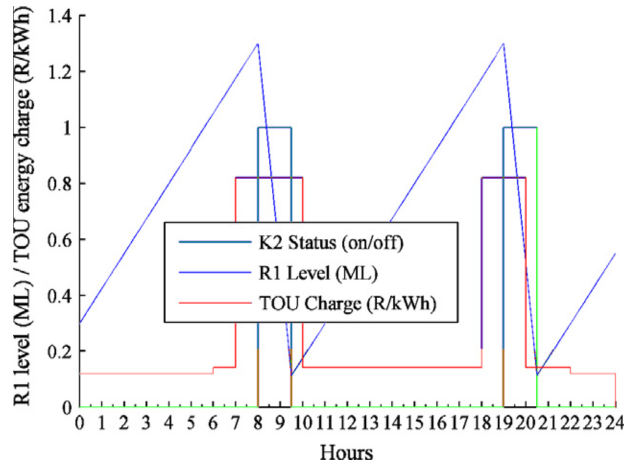

Fig. 6. Current control model for K2 with no optimization on the 30th day.

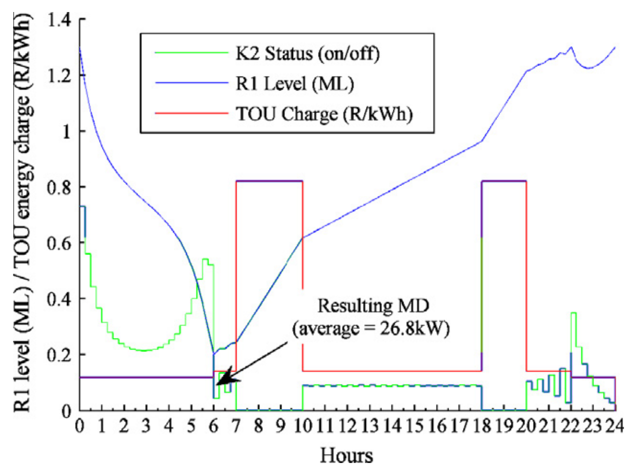

Fig. 7. Open loop optimal control model for K2 with LP optimization ($H = 24$, $S = 2$, timeout = N/A).

(3) *Open loop optimal control model with IP optimization*: The open loop IP optimal control model is simulated over a 30 day period. The reservoir level at the end of each day is used as the initial reservoir level for the next day. Fig. 8 shows the results of the open loop IP optimal control model with $S = 2$ and $H = 24$ on the first day.

The load in Fig. 8 is moved out of the peak periods, and the load in the standard periods is also reduced. The MD is reduced, because K2 runs more frequently, but for shorter times, i.e., only 15 min per 30 min MD period. Note that between 17 h and 18 h K2 runs for two consecutive switching intervals. However, these two switching intervals fall within two separate MD charge periods.

The monthly energy and MD costs for this scenario are shown in Table 4. Fig. 5 (Table 4) shows that this scenario results an MD saving of 3.94% and a TOU energy saving of 1.82% for K2 over 30 days. This gives a total saving (MD and TOU) of 5.76%.

Fig. 8 shows that the optimal control model foresees the approaching peak energy charge periods and reduces the reservoir level to prevent pumping during the peak energy charge periods. This results in an optimal pump schedule, which is difficult to accomplish with a simpler scheduling strategy.

A disadvantage with the pump schedule in Fig. 8 is that K2 is switched on and off unnecessarily in off-peak times, e.g., between 0 h and 6 h. Since the MD charge is not applicable in this period it would be ideal to keep K2 running continuously for longer intervals rather than switching K2 on and off over many short intervals.

(4) *Closed-loop MPC optimal control model with IP optimization*: The closed-loop MPC optimal control model is simulated over a 30 day period. The reservoir level at the end of each switching interval is used as the initial reservoir level for the next switching interval, over the 30 day period.

Fig. 9 shows the results of the closed-loop MPC optimal control model with $S = 2$ and $H = 24$ on the first day. The load is moved out of the peak periods, and the load in the standard periods is also reduced.The MD in Fig. 9 is reduced, because K2 runs more frequently, but for shorter times, i.e., only 15 min per 30 min MD period.

Note that the final reservoir level on the first day in Fig. 9 is lower than the open loop control model for the same scenario in Fig. 8, i.e., 0.6 ML vs. 1 ML. This is caused by the moving control horizon (H) of the closed-loop MPC optimal control model, which means that after each implemented control step the MPC model is optimizing more into the next 24th cycle. In other words, the open loop optimal control model optimizes over the first 24 h only, and will therefore leave the reservoir as full as possible by the end of the cycle to avoid unnecessary pumping. However, the closed-loop MPC optimal control model optimizes the model over each continuous

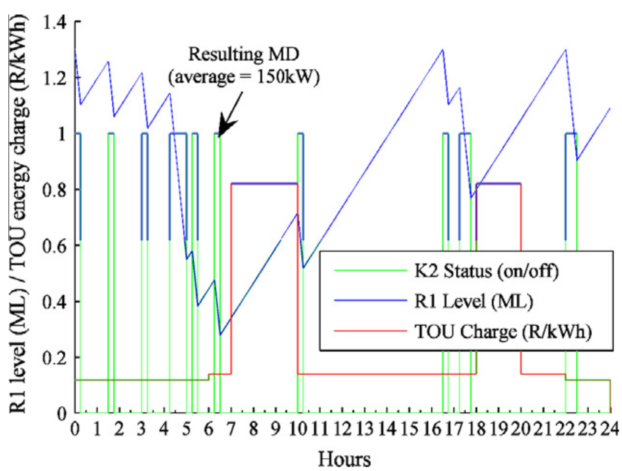

Fig. 8. Open loop optimal control model for K2 with IP optimization (H = 24 h, S = 2, timeout = 10 s).

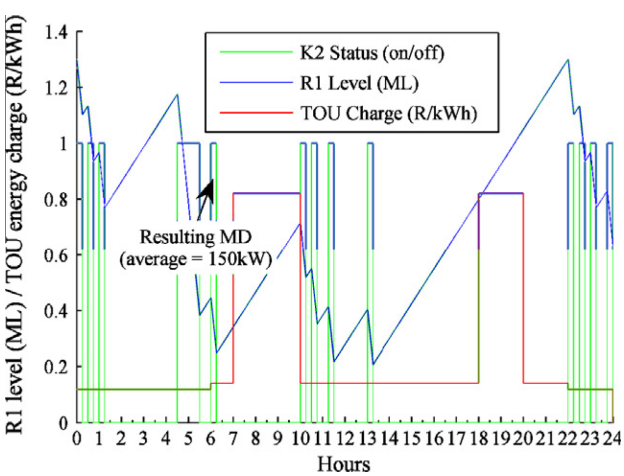

Fig. 9. Closed-loop MPC optimal control model for K2 with IP optimization (H = 24 h, S = 2, timeout = 10 s).

24-h period to cater for any possible system change, which means that a full reservoir at the end of the first 24 h cycle is not seen as optimal by the closed-loop MPC optimal control model.

The monthly energy and MD costs for this scenario are shown in Table 4. Fig. 5 (Table 4) shows that this scenario results in an MD saving of 3.94% and a TOU saving of 1.81% for K2 over 30 days. This gives a total saving (MD and TOU) of 5.75%.

Fig. 5 (Table 4) shows that both the open loop IP control model and the closed-loop MPC control model result in a TOU energy saving of 1.8% and an MD saving of 3.94%. This proves that the closed-loop MPC optimal control model is as good as the open loop optimal control model with IP optimization if there are no disturbances, system model inaccuracies, or plant failures. The effect of disturbances, system model inaccuracies, or plant failures on the control models is evaluated in the next subsection.

Fig. 5 (Table 4) shows that the open loop LP control model results in a similar TOU energy saving of 1.8%, but a higher saving of 7.17% on MD cost. This means that the TOU energy saving of the open loop IP control model and the closed-loop MPC control model can be considered optimal, because the open loop LP control model is used as the benchmark.

It is assumed that the MD saving with the open loop IP control model and the closed-loop MPC control model will converge to the MD saving of 7.17% when more switching intervals per MD period is used i.e. $S > 2$. In other words, a higher switching resolution will enable more, but shorter running intervals. For example, instead of running for a full 15 min ($S = 2$) in the applicable MD period, the pump can run for only 5 min ($S = 6$), which will result in lower MD costs.

It is important to note that the MD saving is larger than the TOU energy saving in the open loop LP control model, the open loop IP control model, and the closed-loop MPC control model.

Note also that the total amount of energy consumed is the same for the current control model, the open loop LP control model, the open loop IP control model, and the closed-loop MPC control model. The electricity cost is only optimized by improving the timing of the energy consumption in the optimal control models.

4.2. Robustness of the closed-loop MPC optimal control model

This subsection evaluates the robustness of the closed-loop MPC optimal control model. The objective of this subsection is to prove that the closed-loop MPC optimal control model compensates for disturbances and model uncertainty in real time, whilst the open loop optimal control model does not.

(1) *Effect of disturbances on the optimal control models*: Fig. 10 shows the results of the open loop optimal control model with IP optimization and the closed-loop MPC optimal control model with a positive random inflow disturbance, i.e., $FLOWIN_t$ is replaced with

$$FLOWIN_t + 0.2 \cdot FLOWIN_t \cdot r(m), \tag{16}$$

where $r(m)$ is a random number between 0 and 1. This means that the constant inflow rate is altered with a random disturbance.

Disturbances in flow rates are common in practical applications that are affected by external factors such as temperature, rain, and equipment age.

Fig. 10 shows that the level of $R1$ exceeds the maximum level constraint (1.3 ML) in the open loop control model, whilst the closed-loop MPC control model compensates for the disturbances and keeps the level of $R1$ within the maximum level constraint.

Note that the switching pattern of the open and closed-loop optimal control models is not exactly the same. This is caused by the moving control horizon (H) of the closed-loop MPC optimal control model, which means that after each implemented control step the MPC model is optimizing more into the next 24th cycle.

Also note that there is not only one unique switching sequence that yields optimal results.

(2) *Effect of an inaccurate system model on the optimal control models*: Fig. 11 shows the results of the open loop optimal control model with IP optimization and the closed-loop MPC optimal control model with an inaccurate outflow model for K2. For demonstration purposes it is assumed that the actual outflow is only 90% of the assumed outflow, i.e.,

$$FLOWOUT_t = 0.9 \cdot 22\ \text{ML}. \tag{17}$$

Inaccurate system models are common in practical applications, because it is likely that the defined plant model will contain some error. The plant model could also be incorrect due to a simplification of the model for practical reasons.

Fig. 11 shows that the level of $R1$ exceeds the maximum level constraint (1.3 ML) in the open loop control model, whilst the closed-loop MPC control model compensates for the inaccurate system model and keeps the level of $R1$ within the maximum level constraint.

(3) *Effect of plant failure on the optimal control models:* Fig. 12 shows the results of the open loop optimal control model with IP optimization and the closed-loop MPC optimal control model with a plant failure. It is assumed that between 12 h and 18 h only one of the G1 to G3 pumps are available for pumping. This means that K2 must compensate with an additional flow of 10 ML/day in this 6 h period.

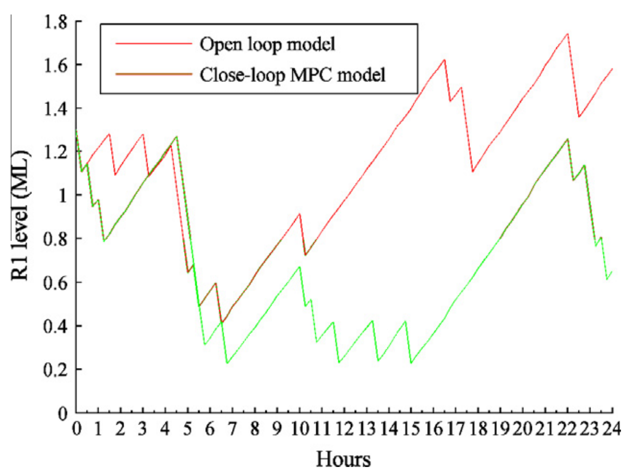

Fig. 10. Reservoir level of the open loop optimal control model with IP optimization and the closed-loop MPC optimal control model with inflow disturbances (H = 24 h, S = 2, timeout = 10 s).

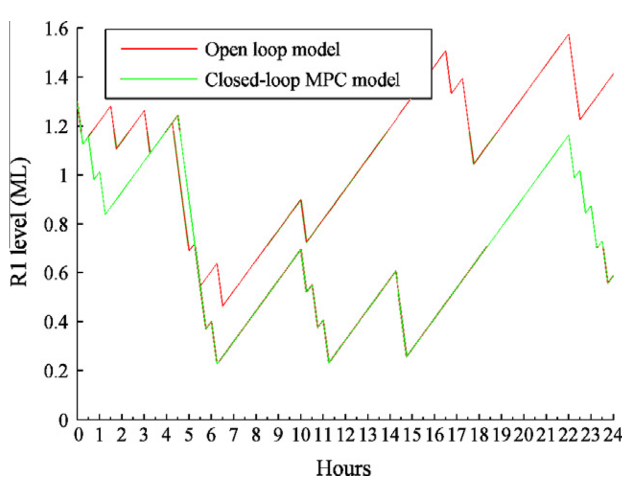

Fig. 11. Reservoir level of the open loop optimal control model with IP optimization and the closed-loop MPC optimal control model with an inaccurate system model (H = 24 h, S = 2, timeout = 10 s).

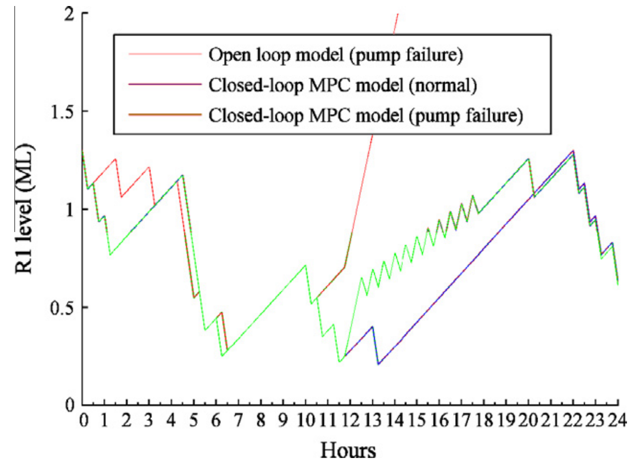

Fig. 12. Reservoir level of the open loop optimal control model with IP optimization and the closed-loop MPC optimal control model with a plant failure disturbances (H = 24 h, S = 2, timeout = 10 s).

Fig. 12 shows that the level of $R1$ exceeds the maximum level constraint (1.3 ML) in the open loop control model, whilst the closed-loop MPC control model compensates for the plant failure and keeps the level of $R1$ within the maximum level constraint. The level of $R1$ for the closed-loop MPC scenario without a plant failure is also shown in Fig. 12. This scenario is included in Fig. 12 to demonstrate exactly how the MPC model compensates for the plant failure, and thereafter returns to the normal switching pattern.

Plant unavailability is common in practical applications, because the entire plant will not always be available due to failures or maintenance outages. Ideally major disturbances like plant failures and outages should automatically feed back to the MPC controller so that the controller can optimize for the new temporary model. This feedback of model changes is also an advantage of a closed-loop MPC model that is not possible with an open loop model.

5. Conclusions and recommendations

This paper defined and evaluated the efficiency of a closed-loop optimal control strategy for load shifting in a plant with TOU and MD charges. The closed-loop optimal control model was implemented with an MPC approach. IP optimization was used to solve the optimization problem, and the water pumping scheme at the water purification plant in Tshwane municipality was selected for the case study.

The closed-loop MPC optimal control model was compared against open loop optimal control models with LP and IP optimization. The LP optimization was included as a benchmark which is considered optimal.

The results showed that the closed-loop MPC optimal control model reduces the TOU energy cost by 1.81%, and the MD cost by 3.94%. This gave a total saving (MD and TOU) of 5.75%. This means that MD optimization had a significant effect on the overall saving.

This result is similar to the saving obtained by the open loop optimal control model with IP optimization. However, the open loop optimal control model with LP optimization resulted in a similar saving on TOU energy cost, but a higher saving of 7.17% on MD cost.

The open loop optimal control model with IP optimization and the closed-loop MPC optimal control model were also simulated with disturbances, an incorrect system model, and a plant failure scenario. The results showed that the open loop control model does not compensate for these disturbances, whilst the closed-loop MPC optimal control model does.

Acknowledgments

The authors would like to thank the anonymous reviewers for their helpful comments. This work is partially supported by the National Research Foundation and the South African National Energy Research Institute.

References

[1] Eskom. Eskom tariffs and charges booklet for 2007/2008. <http://www.eskom.co.za/tariffs>.
[2] Tshwane. Electricity tariffs for Tshwane metropolitan municipality. <http://www.tshwane.gov.za>.
[3] Berg SV, Savvides A. The theory of maximum kW demand charges for electricity. Energy Econ 1983;5:258–66.
[4] Nehrir MH, LaMeres BJ, Gerez V. A customer-interactive electric water heater demand-side management strategy using fuzzy logic. In: IEEE Power Eng Society 1999 winter meetings, vol. 1, February 1999. p. 433–6.
[5] Wu TY, Shieh SS, Jang SS, Liu CCL. Optimal energy management integration for a petrochemical plant under considerations of uncertain power supplies. IEEE Trans Power Syst 2005;20:1431–9.
[6] Ashok S, Banerjee R. An optimization mode for industrial load management. IEEE Trans Power Syst 2001;16:879–84.
[7] Ashok S. Peak-load management in steel plants. Appl Energy 2006;83:413–24.
[8] Zhang J, Xia X. Best switching time of hot water cylinder–switched optimal control approach. In: Proceedings of the 8th IEEE AFRICON conference, Namibia, 26–28 September 2007.
[9] Ashok S, Banerjee R. Load-management applications for the industrial sector. Appl Energy 2000;66:105–11.
[10] Babu CA, Ashok S. Peak load management in electrolytic process industries. IEEE Trans Power Syst 2008;23:399–405.
[11] Jowitt W, Germanopoulos G. Optimal pump scheduling in water-supply networks. J Water Resources Plan Manage 1992;118:406–22.
[12] McCormick G, Powell RS. Optimal pump scheduling in water supply systems with maximum demand charges. J Water Resources Plan Manage 2003;129:372–9.
[13] Yu G, Powell RS, Sterling MJH. Optimised pump scheduling in water distribution systems. J Optim Theory Appl 1994;83:463–88.
[14] Middelberg A, Zhang J, Xia X. An optimal control model for load shifting—with application in the energy management of a colliery. Appl Energy 2009;86:1266–73.
[15] Zhang S, Xia X. Optimal control of operation efficiency of belt conveyor systems. Appl Energy 2010;87:1929–37.
[16] Nitivattananon V, Sadowski EC, Quimpo RG. Optimization of water supply system operation. J Water Resources Plan Manage 1996;122:374–84.
[17] Little KW, McCrodden BJ. Minimization of raw water pumping costs using MILP. J Water Resources Plan Manage 1989;115:511–22.
[18] Bryson Jr AE. Optimal control – 1950 to 1985. IEEE Control Syst Mag 1996;16:26–33.
[19] Brogan WL. Modern control theory. 3rd ed. Upper Saddle River: Prentice-Hall; 1991.
[20] Bemporad A, Borrelli F, Morari M. Model predictive control based on linear programming – the explicit solution. IEEE Trans Autom Control 2002;47:1974–85.
[21] Schrijver A. Theory of linear and integer programming. New York: John Wiley & Sons; 1986.
[22] Xia X, Zhang J, Elaiw A. An application of model predictive control to the dynamic economic dispatch of power generation. Control Eng Practice 2011;19:638–48.
[23] Sivan R, Kwakernaak H. Linear optimal control systems. New York: John Wiley & Sons; 1972.
[24] Zadeh LA. On optimal control and linear programming. IRE Trans Autom Control 1962;7:45–6.
[25] Sallem S, Chaabene M, Kamoun MBA. Energy management algorithm for an optimum control of a photovoltaic water pumping system. Appl Energy 2009;86:2671–80.
[26] Ould-Amrouche S, Rekioua D, Hamidat A. Modelling photovoltaic water pumping systems and evaluation of their CO_2 emissions mitigation potential. Appl Energy 2010;87:3451–9.
[27] Alawaji S, Smiai MS, Rafique S, Stafford B. PV-powered water pumping and desalination plant for remote areas in Saudi Arabia. Fifth Arab International Solar Energy conference. Appl Energy 1995;52:283–9.
[28] Yu Y, Liu J, Wang H, Liu M. Assess the potential of solar irrigation systems for sustaining pasture lands in arid regions – a case study in Northwestern China. Appl Energy 2011;88:3176–82.
[29] Matlab. <http://www.mathworks.com>.
[30] LPSOLVE. <http://lpsolve.sourceforge.net>.
[31] Linderoth JT, Savelsbergh MWP. A computational study of search strategies for mixed integer programming. INFORMS J Comput 1997;11:173–87.